Volume 15, Issue 3, 152530 (1-10)

Iranian Journal of Catalysis (IJC)

https://doi.org/10.57647/j.ijc.2025.1503.30

Green synthesis and characterization of NiO nanoparticles with enhanced sonocatalytic activity

Safaa Ridah Shakor, Saeid Taghavi Fardood*, Ali Naghipour*

Department of Chemistry, Faculty of Science, Ilam University, Ilam, Iran.

*Corresponding authors: s.taghavi@ilam.ac.ir, a.naghipour@ilam.ac.ir

Original Research

Received:
21 February 2025
Revised:
26 April 2025
Accepted:
19 May 2025
Published online:
1 July 2025
Published in issue:
30 September 2025

Abstract:

The persistent nature and environmental toxicity of industrial dyes in wastewater necessitate the development of efficient and sustainable removal technologies, such as sonocatalysis. The sonocatalytic activity of the NiO nanoparticles (NPs) was studied for the degradation of Congo red dye (CR). NiO NPs were prepared via a green method. The obtained NiO NPs were characterized using XRD, BET, TEM, FESEM, EDX, and UV-Vis-DRS. The sonocatalytic efficiency of the NiO NPs was evaluated for the CR degradation. The results show that 95% of CR dye and 56% of total organic carbon (TOC) were removed within 30 min. Nevertheless, when a hydroxyl radical ($^{\bullet}$OH) scavenger t-butanol and hole (h^{+}) scavenger (EDTA) were added it was observed that degradation efficiency reduced from 95% to 52% and 64% respectively, which revealed that $^{\bullet}$OH is the main oxidizing agents in this process. LC-MS analysis identified degradation products and enabled the proposal of a plausible sonocatalytic degradation pathway for Congo red dye. NiO NPs' reusability was evaluated using the same reaction conditions for five consecutive cycles. However, a slight loss of sonocatalytic efficiency was obtained, illustrating the stability and reusability of the nanoparticles.

Keywords: Dye degradation; Green method; NiO nanoparticles; Sonocatalysis

1. Introduction

Nanotechnology has made significant gains in producing nanoparticles with precise size and morphology for certain purposes. Nanotechnology is being studied in various sectors, from medical to environmental protection [1–3]. Nanoparticles (NPs) have a size, distribution, and shape. Due to their many unique, surprising, and intriguing properties, nanoparticles have many applications [4–7]. The goal is to improve methods for synthesizing NPs with specific size, shape, composition, and well-ordered dispersity to improve their physical, chemical, optical, and catalytic properties for environmental and sonocatalytic applications [8–12]. The significance of biofunctional nanoparticle synthesis has attracted the interest of numerous research groups, leading to a rapidly expanding field [13–16]. Researchers have used cost-effective methods to synthesize metal oxide nanoparticles for various applications to meet the growing need for eco-friendly nanoparticles [17–19]. Although physical and chemical approaches are widely utilized for the preparation of NPs, physical methods are generally expensive, and chemical methods can be detrimental to both the environment and living organisms [20–22]. Numerous studies have suggested using plants and natural gels for nanoparticle synthesis [23–26]. Green synthesis, formerly known as bio materials innovation, is a cost-effective, environmentally friendly, and favored approach to chemical and physical processes. Ongoing efforts aim to enhance nanoparticles' quality, size, shape, and catalytic activity by drawing inspiration from biological processes. The green synthesis of nanoparticles has utilized both natural and synthetic products as reducing and capping agents [27–32]. Nickel oxide (NiO) nanoparticles (NPs) are regarded as prototypical p-type semiconductors with a band gap energy ranging from 3.6 to 4.9 eV [33]. Their high surface area contributes to their exceptional photocatalytic and environmental remediation properties [34–37]. Their biocompatibility and low toxicity make them an exceptional material for various applications [38–40]. As a result, this substance has attracted considerable interest from scientists in recent times and has been extensively applied in various fields, including sensors, photocatalysis, and sonocatalysis [41–43]. Addi-

tionally, NiO NPs have been shown to be efficient adsorbents for removing toxic pollutants and dyes [44, 45]. Other sonocatalysts, such as CdO, ZnO, CeO_2, and CuO, exhibit promise in degrading organic contaminants, demonstrating adaptability and efficiency in environmental applications [46–49]. Recent studies demonstrate that sonocatalysis improves the degradation efficiency of specific materials. The increasing focus on these catalysts underscores their importance in addressing environmental issues, such as water pollution [50, 51]. The sonocatalytic process depends on sonoluminescence and hot spots from US cavitation, which refers to the formation, growth, and collapse of microbubbles in an aqueous solution. Local "hot spots" generate intense heat and pressure that can elevate semiconductor sonocatalyst electrons from the valence band (VB) to the conduction band (CB). Moreover, sonoluminescence resulting from the collapse of cavitation bubbles can activate the sonocatalyst to generate electron-hole pairs (e^-–h^+) [52]. Sonoluminescence and hot spots can also dissociate water molecules into small amounts of hydrogen and hydroxyl radicals ($^\bullet$H and $^\bullet$OH). The efficient utilization of semiconductor sonocatalysts is therefore imperative and urgent [53]. CR dye (Fig. 1) is a harmful organic contaminant that has raised concerns recently [54–56]. This work involved the synthesis of NiO NPs through an eco-friendly method, followed by characterization of their properties using various analytical techniques. Finally, CR dye photodegradation was studied under various conditions.

2. Experimental

2.1 Materials

The tragacanth gum (TG) was obtained from a nearby natural products store. The $Ni(NO_3)_2{\cdot}6H_2O$, Tert-butyl alcohol (t-butanol) (≥99%), benzoquinone (BQ) (≥ 98%), and Ethylenediamine tetra acetic acid (EDTA, ≥ 99%) were purchased from Merck and Sigma-Aldrich. Congo red dye ($C_{32}H_{22}N_6Na_2O_6S_2$, Sodium 3,3'-([1,1'-biphenyl]-4,4'-diylbis(diazene-2,1-diyl))bis(4 aminonaphthalene-1-sulfonate) was acquired from Alvan Sabet Co (Iran).

2.2 Characterization

The X-ray diffraction (XRD) of NiO NPs were examined with an advanced X'Pert PRO diffractometer. A TESCAN MIRA 30 with energy dispersive X-ray (EDX) and an EM 208S were used for field emission scanning electron microscope (FESEM), EDX and transmission electron microscope (TEM) analysis. The produced solutions' optical absorption spectra were recorded by a Cary Series spectrophotometer. Belsorp Mini II and ultraviolet-visible diffuse reflectance spectroscopy (UV-vis DRS) (Shimadzu UV-2550, Japan) analysers measured surface area and optical characteristics. Shimadzu's TOC-5000 was used to measure total organic carbon (TOC). Liquid chromatography-mass spectrometry (LC-MS) was performed using a Waters 2695 HPLC-MS system.

2.3 Synthesis of NiO NPs

The NiO nanoparticles were prepared using an environmentally friendly method [29]. Initially, TG was dissolved in distilled water for 45 min at 70 °C to form a gel. Then, 1.5 g of $Ni(NO_3)_2{\cdot}6H_2O$ were added to the gel, and the mixture was heated at 75 °C for 12 hours with continuous stirring. The resulting dry gel was subsequently annealed at 500 °C for 4 hours to produce NiO nanoparticles.

2.4 Sonodegradation of CR dye

The CR degradation was studied using NiO NPs as a catalyst in an ultrasonic cleaner, operating at 200 W. The temperature was kept stable during the entire process. To identify the best conditions for degradation, a range of CR concentrations (10 – 40 mg/L), different amounts of NiO (10 – 40 mg), and various contact times were employed under ultrasonic irradiation. After separation of the NiO NPs, the degradation performance and UV-Vis spectrum of the CR solution were assessed using a UV-Vis instrument. The CR concentration was measured by absorbance at 499 nm. The equation below can be employed to determine the degradation efficacy:

$$\text{Degradation } (\%) = \left(\frac{A_0 - A}{A_0}\right) \times 100$$

where A_0 represents the initial absorbance of the dye, and A denotes the absorbance remaining after exposure to visible light irradiation.

3. Results and discussion

3.1 Characterization of NiO NPs

The XRD pattern of green synthesized NiO NPs has been displayed in the figure 2. The diffraction peaks exhibit clear and precise characteristics that correspond to the cubic structure. The crystal planes of the NiO NPs have been indexed as (111), (200), (220), (311), and (222), which closely match the JCPDS Card No: 75-0197. The strong intensity

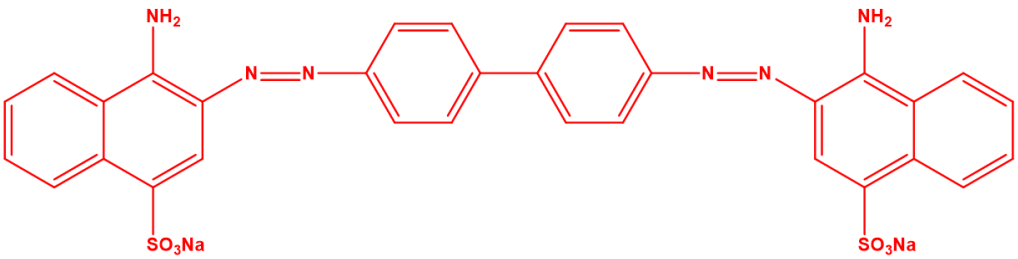

Figure 1. Chemical Structure of CR dye.

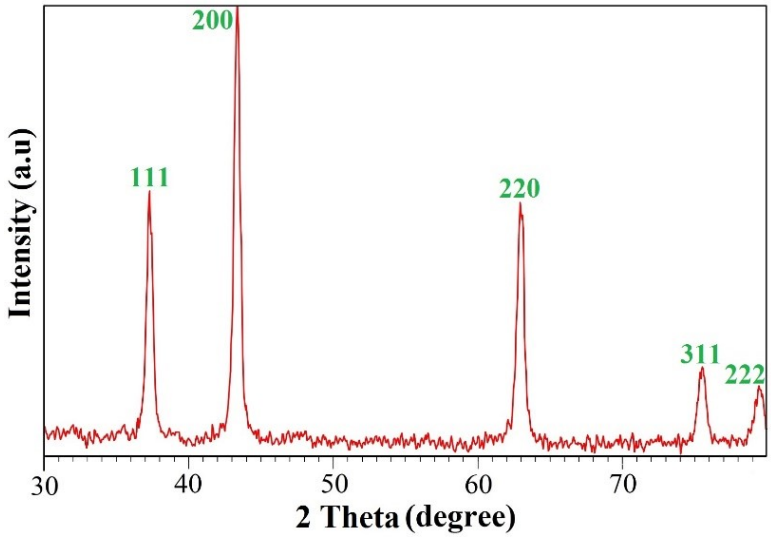

Figure 2. XRD pattern of the NiO NPs.

and clarity of the peaks provide additional evidence of the crystallinity of the NiO NPs. The average crystallite size of the NiO NPs was determined to be approximately 19 nm using the Debye-Scherrer equation [57, 58].

The FESEM and TEM images in figure 3a, 3b illustrate the morphology and particle size of NiO NPs. From the analysis of the FESEM image, it is clear that the NiO nanoparticles display a uniform spherical shape and are uniformly distributed. The TEM image gives additional data suggesting that the NiO NPs have an approximate size of 25 nm. The EDX analysis (figure 3c) was used to determine the chemical elements of the NiO NPs. The EDX analysis revealed

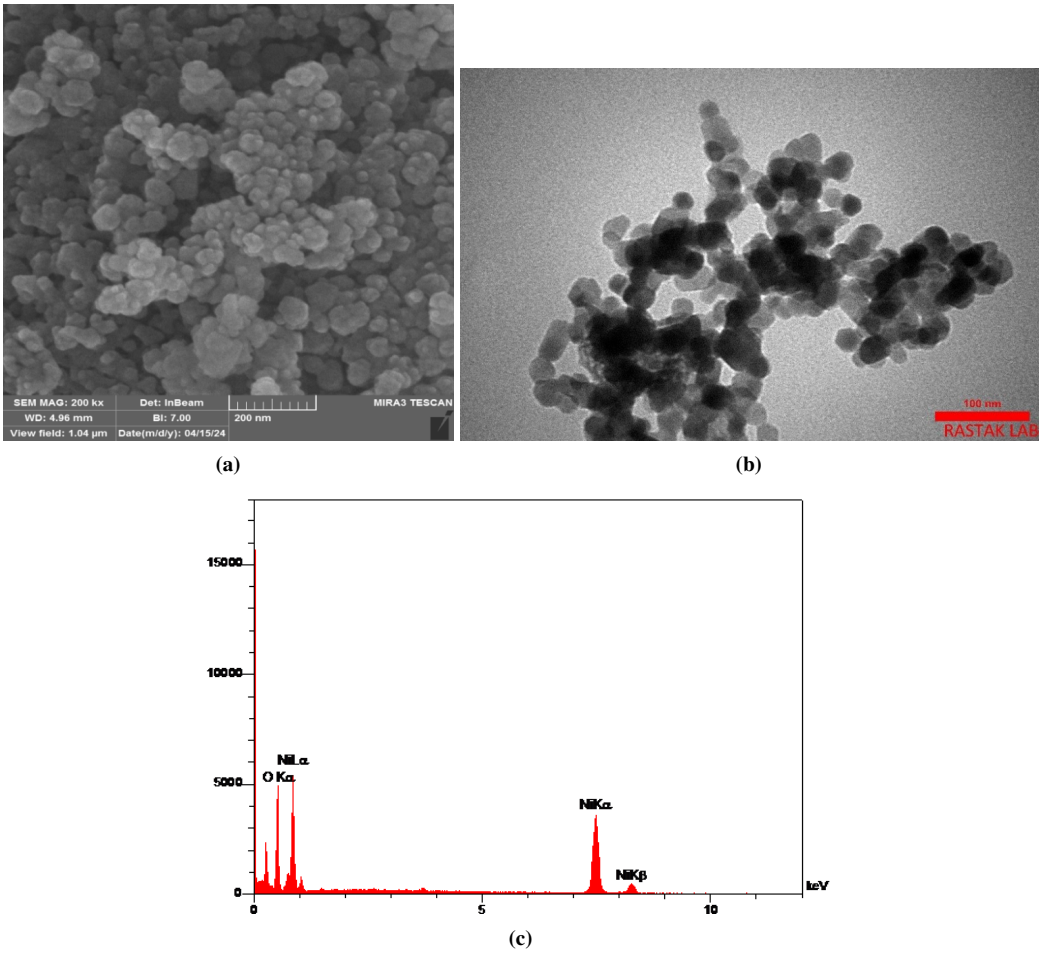

Figure 3. (a) FESEM, (b) TEM, and (c) EDX images of NiO NPs.

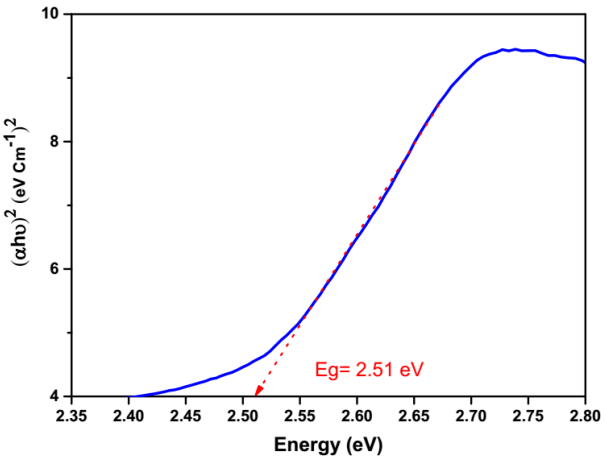

Figure 4. Tauc plot of NiO.

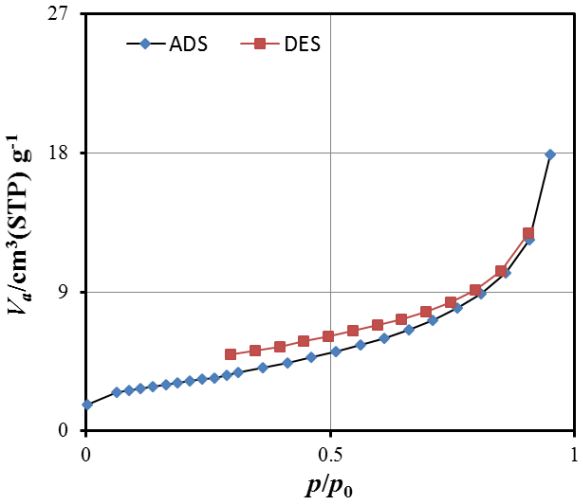

Figure 5. The N_2 adsorption-desorption curve of the NiO NPs.

peaks for nickel and oxygen, confirming the composition.

The tauc plot of the NiO NPs is shown in Fig. 4. The plot indicates that the band gap of NiO is approximately 2.51 eV. Similar results have been reported in other studies as well [59, 60]. This result indicates that the NiO NPs have an appropriate band gap for the dye degradation under visible light. The observed substantial red shift in the band, compared to that reported for bulk NiO ($\sim 3.6-4.9$ eV) [61], could be attributed to the strong p–d exchange interaction between Ni-3d and O-2p orbitals.

The CB and VB potentials of NiO NPs were calculated using the following equations [62–65]:

$$E_{\mathrm{VB}} = X - E_e + 0.5E_g$$

$$E_{\mathrm{CB}} = E_{\mathrm{VB}} - E_g$$

where X is the absolute electronegativity of the semiconductor (5.75 eV for NiO), E_e is the energy of free electrons on the hydrogen scale (~ 4.5 eV), and E_g is the band gap energy of the NiO. Based on these values, the CB and VB of NiO were estimated to be approximately 0.004 eV and 2.514 eV, respectively.

The BET method was used to evaluate the active surface area of NiO NPs. The specific surface area, the pore diameter, and the total pore volume of the NiO NPs were found to be 41.226 m^2/g, 9.874 nm, and 0.0277 cm^3/g, respectively. The N_2 absorption/desorption isotherm, presented in figure 5, verifies the characteristic Type IV behavior in accordance with the IUPAC classification of materials [66, 67].

3.2 Sonocatalytic efficiency of NiO NPs

The sonocatalytic activity of NiO NPs was assessed by degrading Congo red dye at natural pH. The degradation process was monitored by tracking the variation in the absorbance peak of Congo red around 449 nm.

As demonstrated in figure 6a, when the catalyst dosage is raised from 10 to 30 mg with constant irradiation time, the degradation efficiency is observed to improve. This was attributed to the enhancement of active sites and •OH radicals by the presence of the catalysts in the degradation of dye. However, when the NiO dosage increases from 30 to 40 mg, the degradation efficiency slightly reduces. When the doses of sonocatalyst are increased, an aggregation of particles occurs, which in turn reduces the total surface area and active sites to generate •OH radicals. Furthermore, the use of a high concentration of sonocatalyst can hinder the process of cavitation by minimizing the ultrasonic waves that would help in the formation of cavitation bubbles in the solution [68].

Figure 6b illustrates the impact of initial CR amount on sonodegradation, with dye concentrations varying between 10 and 40 mg/L, constant NiO dosage (30 mg), and contact time (30 min). As anticipated, degradation efficiency gradually decreased with higher dye concentration. Increasing the dye concentration to 40 mg/L achieved an 81% degradation of CR. High dye concentrations lead to excessive adsorption on the catalyst surface, which hinders heat and energy absorption from acoustic cavitation, reducing hydroxyl radicals and degradation efficiency [69].

The sonocatalytic performance of NiO for CR dye degradation was evaluated by determining the efficiency under three experimental conditions: Sonolysis, adsorption (NiO in the dark), and sonocatalysis (NiO under US irradiation). No degradation of the CR dye was found in the sonolysis conditions. Under adsorption conditions, 53% of the CR dye was eliminated. However, as shown in figure 6c, 95% of the CR dye was degraded in just 30 minutes during sonocatalysis.

To identify the optimal duration of the sonocatalyst process, the experiment was carried out with a fixed amount of NiO and CR concentration at different times. The results obtained are shown in figure 6d. The absorption spectrum of the degradation is shown by the decrease of the maximum absorption values with time under ultrasonic irradiation. Under optimal conditions, 95% of the CR dye was destroyed in 30 min. TOC removal from CR dye was analyzed prior to and following the degradation test under identical conditions. The results showed that 56% of the TOC was removed within 30 min. The rapid and efficient degradation of CR dye under ultrasonic irradiation clearly demonstrates the sonocatalytic capability of the obtained NiO NPs. The en-

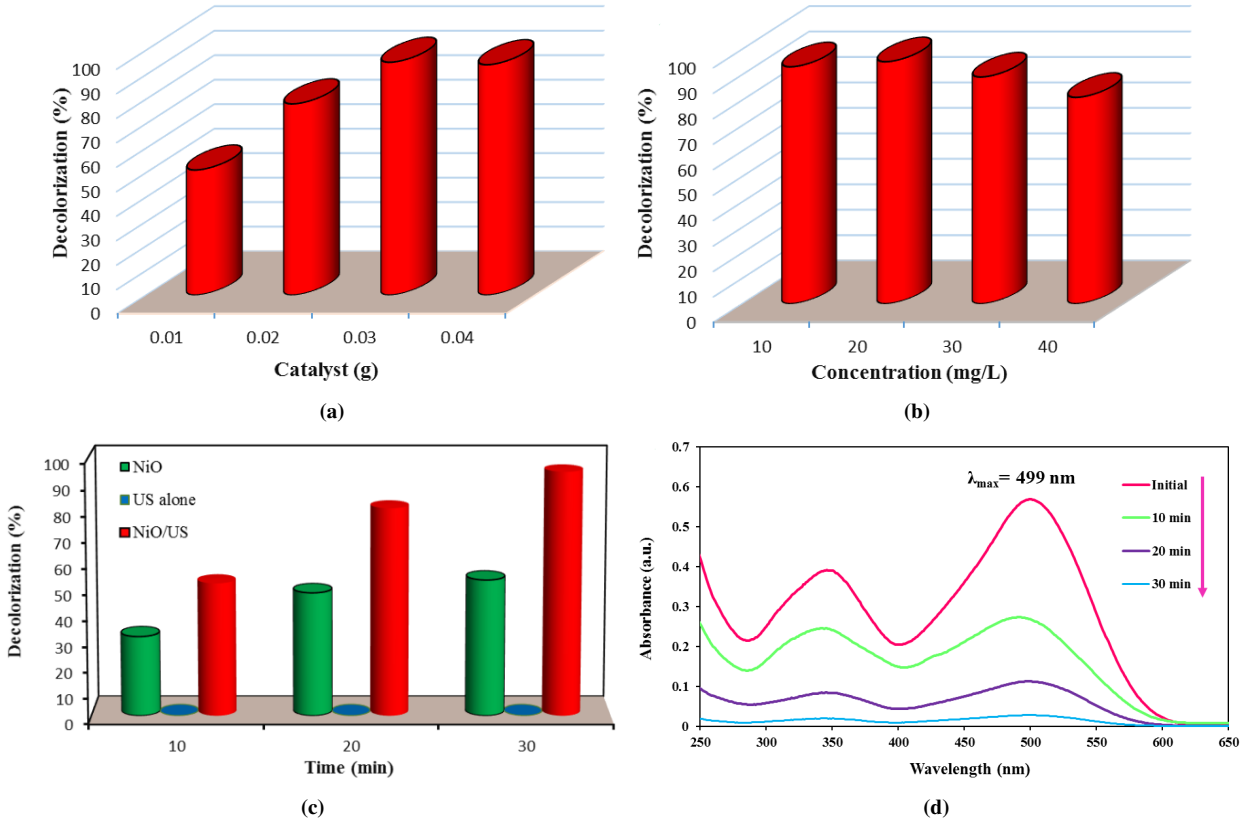

Figure 6. The Effect of (a) NiO Dosage (20 ppm CR, 30 min) (b) CR Concentration (0.03 g NiO, 30 min) (c) Ultrasonic irradiation (0.03 g NiO, 20 ppm of CR) (d) UV-Vis spectra of sonocatalytic degradation (0.03 g NiO, 20 ppm CR).

hanced sonocatalytic efficiency of NiO NPs is primarily attributed to their high crystallinity, uniform particle size (∼ 25 nm), narrow band gap (∼ 2.51 eV), deep valence band (∼ 2.514 eV), and excellent sonocatalytic activity under ultrasonic conditions.

Scavenger experiments revealed the active oxidant species and clarified the sonodegradation process [70]. Figure 7 shows that the introduction of t-butanol, a scavenger for hydroxyl radicals (•OH), reduced CR degradation efficiency to 52% after 30 minutes. This suggests that sonocatalysis is reliant on •OH radicals. EDTA, acting as a hole (h^+) quencher, reduced CR degradation to 64%, indicating that

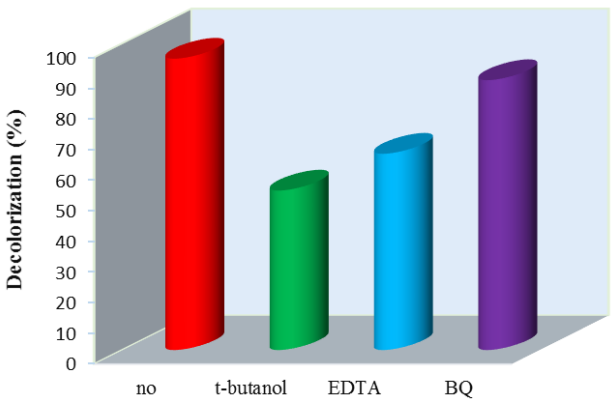

Figure 7. Influence of scavenging agents on CR dye degradation (20 ppm CR, 0.03 g NiO, 30 min).

•OH radicals play a more dominant role in the process. The use of p-benzoquinone (BQ) as an $O_2^{\bullet-}$ scavenger had a minimal effect on degradation. These results confirm that, although h^+ contributes to degradation in this system, •OH radicals are the primary active agents [71–73]. The suggested pathway for the degradation of CR dye, as illustrated by LC-Mass analysis, is presented in figure 8. The findings indicate that the molecules of the CR dye undergo degradation, resulting in the formation of smaller fragments. The fragmented molecules are presented in Table 1, located further down, providing insight into the sequential breakdown steps and supporting the proposed degradation mechanism.

An important advantage of using nanoparticles in water purification is their ability to be reused multiple times [74]. The stability and sonocatalytic efficiency of NiO NPs were investigated in five consecutive experiments under the optimal conditions. The sonocatalyst from each experiment was centrifuged, rinsed with distilled water, and reused to assess its reusability. The results, as shown in figure 9, indicated a minor decline in degradation efficiency even after five cycles of recycling.

A comparison of the degradation of CR using other catalysts was performed. Table 2 describes the comparison of NiO NPs as a unique sonocatalyst for CR degradation. This report is among the first studies to show that NiO NPs exhibit the highest sonodegradation efficiency for CR dye. This technique produces NiO nanoparticles through a green synthesis method, which are used as sonocatalysts and show promise for the degradation of organic pollutants.

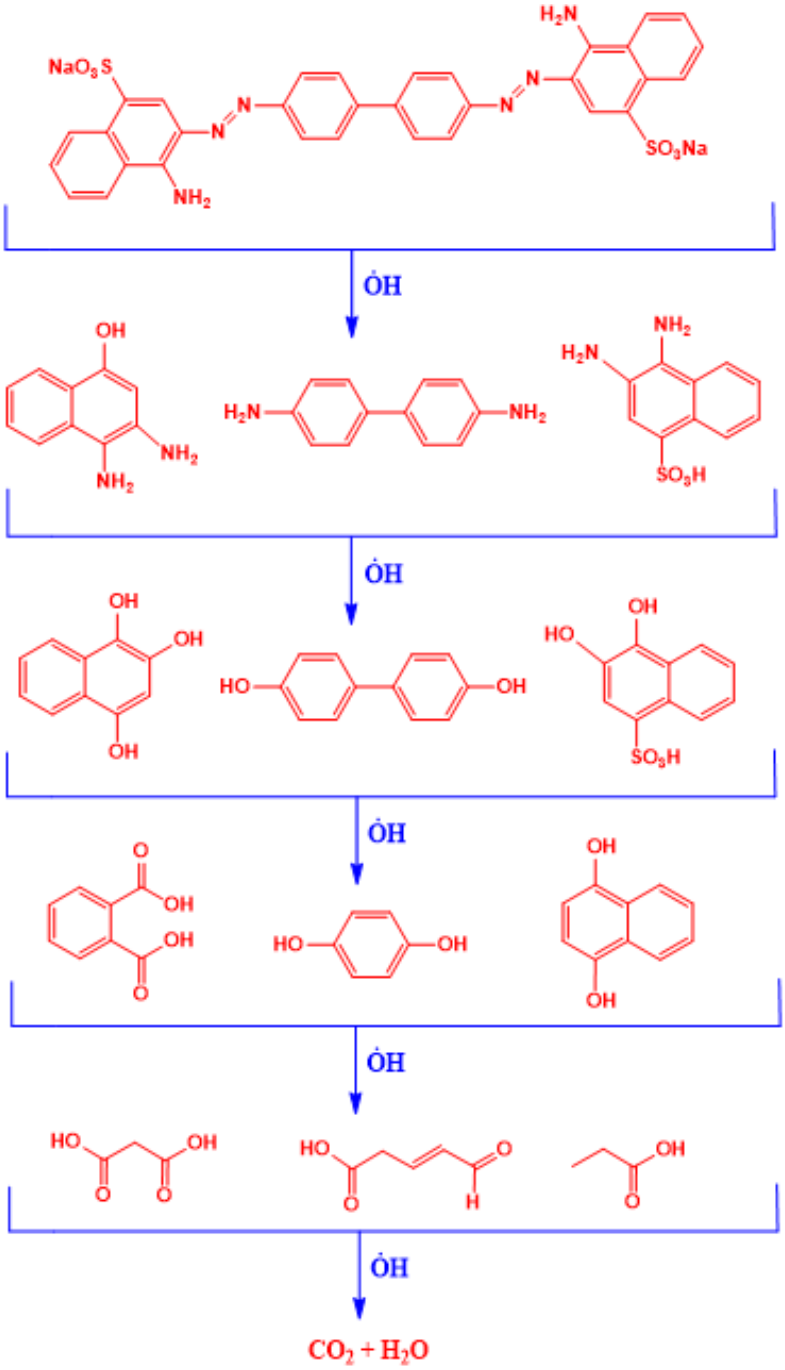

Figure 8. Proposed Sonocatalytic Degradation Pathway of CR dye.

4. Conclusion

This work demonstrates that NiO nanoparticles synthesized via a green method show strong sonocatalytic activity for Congo red dye degradation. The characterization of NiO through various advanced techniques confirmed its structural and chemical properties. FESEM and TEM images showed that NiO nanoparticles have a uniform spherical shape and an average size of 25 nm. The Tauc plot revealed a band gap of 2.51 eV, and BET analysis showed a specific surface area of 41.226 m^2/g, highlighting the NiO NPs' potential as an efficient sonocatalyst. The sonocatalytic performance of NiO was remarkable, achieving 95% removal of Congo red dye and a 56% reduction in TOC within 30 min under ultrasonic irradiation. •OH radicals play a key role in degradation, as the use of t-butanol, a •OH scavenger, reduced the degradation from 95% to 52%, confirming that •OH radicals are the primary oxidants in sonocatalysis. LC-MS analysis confirmed the formation of several degradation products, supporting the proposed degradation pathway. Furthermore, recycling experiments showed that NiO nanoparticles exhibit good reusability and stability. Given their excellent sonocatalytic performance, NiO is recognized as a promising candidate for water remediation. This study provides valuable insights into developing highly efficient sonocatalysts for environmental applications.

Table 1. Identified intermediates from CR sonodegradation by LC-MS.

No	Structure	m/z	No	Structure	m/z
1		238	2	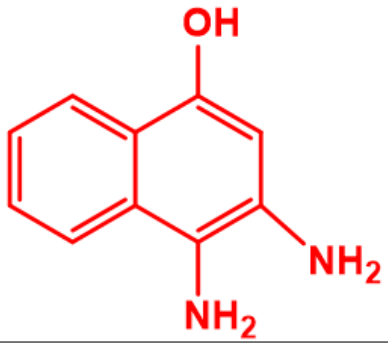	174
3	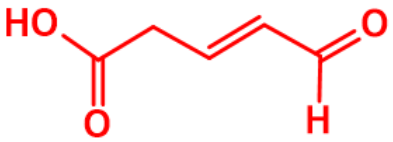	114	4		110
5	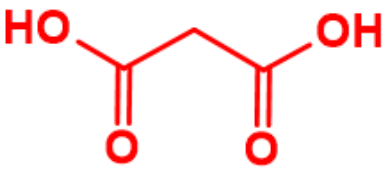	104	6	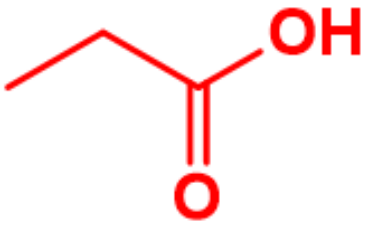	74

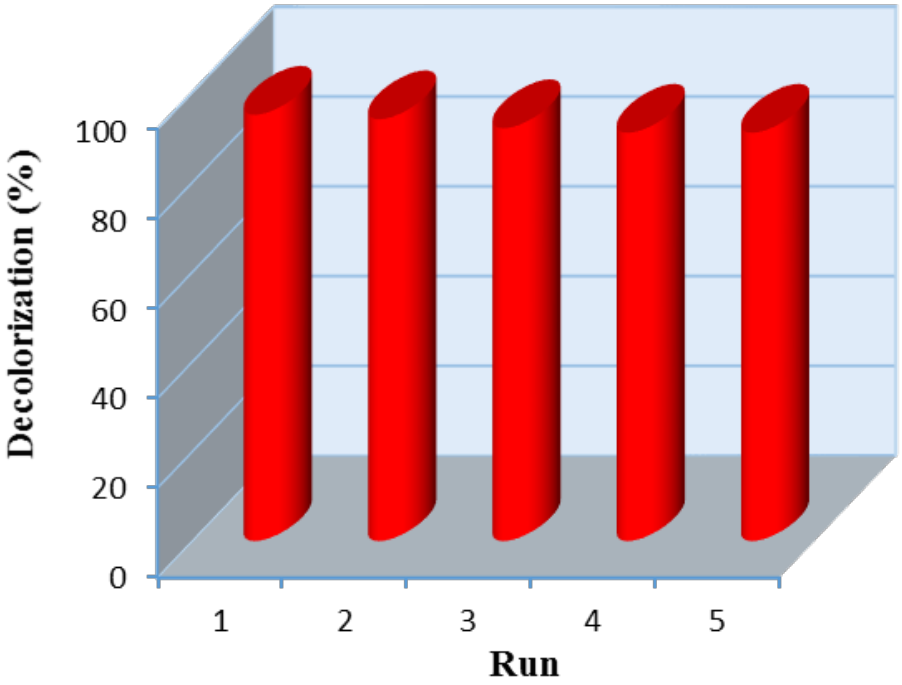

Figure 9. Recyclability of NiO NPs (0.03 g NiO, 20 ppm CR).

Table 2. Comparison of catalytic performance in CR degradation.

Catalysts	Degradation method	Time (min)	Degradation performance (%)	Refs.
TiO_2	Sonocatalysis	180	80	[75]
NiO	Photocatalysis	160	84	[76]
$Mg_{0.5}Co_{0.5}Fe_2O_4$	Photocatalysis	30	93	[77]
CeO_2-500	Photocatalysis	100	76.44	[62]
CdO-NiO	Photocatalysis	140	90.18	[36]
NiO	Photocatalysis	140	87.81	[36]
Cellulose/TiO_2	Sonocatalysis	30	48	[78]
$MgFe_2O_4$@CeO_2	Photocatalysis	60	93	[79]
NiO	**Sonocatalysis**	**30**	**95**	**This work**

Authors contributions
Authors have contributed equally in preparing and writing the manuscript.

Availability of data and materials
The data that support the findings of this study are available from the corresponding author, upon reasonable request.

Conflict of interests
The author declare that they have no known competing financial interests or personal relationships that could have appeared to influence the work reported in this paper.

References

[1] M. B. Al Taee and B. M. Al Shabander. *Chem. Methodol.*, **6** (2022): 831–841.
DOI: https://doi.org/10.22034/chemm.2022.352379.1578.

[2] M. A. Turkia and T. A. Salman. *J. Chem. Rev.*, **6** (2024):458–481.
DOI: https://doi.org/10.48309/jcr.2024.468135.1350.

[3] A. R. Faraji, A. Ramazi Farahani, N. Bakhsi Khoramdareh, A. Gil, S. Jafari, Z. Hekmatian, and N. Shojaei. *J. Environ. Chem. Eng.*, **11** (2023):111348.
DOI: https://doi.org/10.1016/j.jece.2023.111348.

[4] H. R. Rahman, H. B. Abdulrahman, and R. B. Abdulrahman. *Baghdad Science Journal*, **22** (2025).
DOI: https://doi.org/10.21123/bsj.2024.9346.

[5] S. F. Talebi, P. Mohammadparast-Tabas, S. A. Hosseini, A. Shahriari, M. Zare-Bidaki, S. F. Askari, M. Yousefi, and M. Sedighi. *Results in Chemistry*, **10** (2024):101741.
DOI: https://doi.org/10.1016/j.rechem.2024.101741.

[6] A. Nezamzadeh-Ejhieh and Z. Salimi. *Desalination*, **280** (2011): 281–287.
DOI: https://doi.org/10.1016/j.desal.2011.07.021.

[7] S. Badkoobeh Hezaveh, M. T. Ranjbar, and B. Nabavi. *Colloid Nanosci. J.*, **2** (2024):228–237.
DOI: https://doi.org/10.61186/cnj.2.1.228.

[8] Y. Min, K. Zhang, Y. Chen, and Y. Zhang. *Ultrason. Sonochem.*, **19** (2012):883–889.
DOI: https://doi.org/10.1016/j.ultsonch.2011.12.015.

[9] K. K. Veni, L. Nehru, R. Kavitha, and S. Sagadevan. *Surfaces and Interfaces*, **51** (2024):104590, .
DOI: https://doi.org/10.1016/j.surfin.2024.104590.

[10] E. Hadi and K. K. Jasim. *Adv. J. Chem. A*, (2024):604–614.
DOI: https://doi.org/10.48309/ajca.2025.474706.1654.

[11] E. Takele Assefa, G. Shumi, K. Mohammed Gendo, G. Kenasa, and N. Roba. *Results in Chemistry*, **8** (2024):101606.
DOI: https://doi.org/10.1016/j.rechem.2024.101606.

[12] S. Venkatesan, S. Suresh, J. Arumugam, P. Ramu, N. Pugazhenthiran, R. Jothilakshmi, and K. M. Prabu. *Results in Chemistry*, **7** (2024): 101315.
DOI: https://doi.org/10.1016/j.rechem.2024.101315.

[13] F. Moradnia, S. Taghavi Fardood, and A. Ramazani. *Appl. Organomet. Chem.*, **38** (2024):e7315, .
DOI: https://doi.org/10.1002/aoc.7315.

[14] J. Shubha, H. Savitha, R. Patil, M. E. Assal, M. R. Shaik, M. Kuniyil, O. Alduhaish, N. Dubasi, and S.F. Adil. *J. King Saud Univ. Sci.*, **35** (2023):102784.
DOI: https://doi.org/10.1016/j.jksus.2023.102784.

[15] S. Dichayal, V. Murade, S. Deshmukh, S. Pansambal, D. Hase, and R. Oza. *J. Chem. Rev.*, **6** (2024):514–531.
DOI: https://doi.org/10.48309/jcr.2024.471812.1361.

[16] Z. Sabouri, S. Sammak, S. Sabouri, S. S. Tabrizi Hafez Moghaddas, and M. Darroudi. *Chem. Methodol.*, **8** (2024):164–176.
DOI: https://doi.org/10.48309/chemm.2024.436507.1758.

[17] B. K. Mandal, R. Mandal, S. Sikdar, S. Sarma, A. Srinivasan, S. R. Chowdhury, B. Das, and R. Das. *Materials Today Communications*, **34** (2023):105302, .
DOI: https://doi.org/10.1016/j.mtcomm.2022.105302.

[18] S. Hussain, M. Ali Muazzam, M. Ahmed, M. Ahmad, Z. Mustafa, S. Murtaza, J. Ali, M. Ibrar, M. Shahid, and M. Imran. *J. Taibah Univ. Sci.*, **17** (2023):2170162.
DOI: https://doi.org/10.1080/16583655.2023.2170162.

[19] L. Yadeta Gemachu and A. Lealem Birhanu. *Green Chem. Lett. Rev.*, **17** (2024):2293841.
DOI: https://doi.org/10.1080/17518253.2023.2293841.

[20] N. Venkatalakshmi, H. J. Kini, and H.B. Naik. *Inorg. Chem. Commun.*, **151** (2023):110490.
DOI: https://doi.org/10.1016/j.inoche.2023.110490.

[21] U. O. Aigbe and A. O. Osibote. *J. Hazard. Mater. Adv.*, **13** (2024): 100401.
DOI: https://doi.org/10.1016/j.hazadv.2024.100401.

[22] A. Nezamzadeh-Ejhieh and Z. Shams-Ghahfarokhi. *J. Chem.*, **2013** (2013):104093.
DOI: https://doi.org/10.1155/2013/104093.

[23] M. A. Islam, V. Selvanathan, P. Chelvanathan, M. M. Haque, M. Mottakin, I. A. Alnaser, M. R. Karim, M. A. Ibrahim, T. Suemasu, and M. Akhtaruzzaman. *J. Sol-Gel Sci. Technol.*, **109** (2024):580–593. DOI: https://doi.org/10.1007/s10971-023-06296-3.

[24] S. Taghavi Fardood, A. Ramazani, and S. Moradi. *Chem. J. Mold.*, **12** (2017):115–118, . DOI: https://doi.org/10.19261/cjm.2017.383.

[25] V. Selvanathan, M. A. Islam, T. S. Kiong, S. A. Razali, H. F. Alharbi, and M. Akhtaruzzaman. *Ceram. Int.*, **50** (2024):10843–10853. DOI: https://doi.org/10.1016/j.ceramint.2023.12.400.

[26] M. A. Abdelwahab, A. Nabil, H. El-Hosainy, R. Tahway, and M. S. Taha. *Results in Chemistry*, **7** (2024):101274. DOI: https://doi.org/10.1016/j.rechem.2023.101274.

[27] G. preet Singh, K. Singh, K. Chandel, P. Kaur, and J. Kaur. *Inorg. Chem. Commun.*, **157** (2023):111250. DOI: https://doi.org/10.1016/j.inoche.2023.111250.

[28] S. Taghavi Fardood, F. Moradnia, F. Yekke Zare, S. Heidarzadeh, M. Azad Majedi, A. Ramazani, M. Sillanpää, and K. Nguyen. *Sci. Rep.*, **14** (2024):6755, . DOI: https://doi.org/10.1038/s41598-024-56666-2.

[29] M. T. Kiani, A. Ramazani, and S. Taghavi Fardood. *Appl. Organomet. Chem.*, **37** (2023):e7053. DOI: https://doi.org/10.1002/aoc.7053.

[30] R. A. Ahmed, O. H. Salah, R. R. Abass, M. M. Karim, S. A. Khuder, S. Ahjel, and I. I. Dawood. *Asian J. Green Chem.*, **8** (2024):308–318. DOI: https://doi.org/10.48309/ajgc.2024.449143.1487.

[31] M. Mehdi Zabihi, S. Eghbaliferiz, M. Khorashadizadeh, S. Mortazavi-Derazkola, and M. Yousefi. *Results in Chemistry*, **7** (2024):101510. DOI: https://doi.org/10.1016/j.rechem.2024.101510.

[32] A. B. Pebdeni, C. A. Khurshid, S. D. Abkenar, and M. Hosseini. *ChemistrySelect*, **6** (2021):5034–5042. DOI: https://doi.org/10.1002/slct.202101116.

[33] D. C. Onwudiwe, N. H. Seheri, L. Hlungwani, H. Ferjani, and R. Rikhotso-Mbungela. *J. Mol. Struct.*, **1317** (2024):139084. DOI: https://doi.org/10.1016/j.molstruc.2024.139084.

[34] D. Borah, P. Saikia, D. Gogoi, A. Das, J. Rout, N. N. Ghosh, P. Pandey, M. D. Gupta, and C. R. Bhattacharjee. *Inorg. Chem. Commun.*, **156** (2023):111182. DOI: https://doi.org/10.1016/j.inoche.2023.111182.

[35] A. E. Ferenji, Y. E. Hassen, S. L. Mekuria, and W. M. Girma. *Heliyon*, **10** (2024). DOI: https://doi.org/10.1016/j.heliyon.2024.e31669.

[36] R. K. Mandal, A. S. Mondal, S. Ghosh, A. Halder, and T. P. Majumder. *Results in Chemistry*, **5** (2023):100810, . DOI: https://doi.org/10.1016/j.rechem.2023.100810.

[37] S. Prabhu, T. Daniel Thangadurai, P. Vijai Bharathy, and P. Kalugasalam. *Results in Chemistry*, **4** (2022):100285. DOI: https://doi.org/10.1016/j.rechem.2022.100285.

[38] S. Bavaji and A.J. Ahamed. *Chem. Phys. Impact*, **8** (2024):100647. DOI: https://doi.org/10.1016/j.chphi.2024.100647.

[39] S. Pramila, V. Lakshmi Ranganatha, G. Nagaraju, and C. Mallikarjunaswamy. *Inorg. Nano-Metal Chem.*, **53** (2023):527–538. DOI: https://doi.org/10.1080/24701556.2022.2081188.

[40] F. Allawi Abdul Sajad, H. K. Egzar, and M. A. Mahdi. *Iran. J. Catal.*, **13** (2023). DOI: https://doi.org/10.30495/ijc.2023.1987426.2010.

[41] M. Choolaei, Q. Cai, and B. A. Horri. *Ceram. Int.*, **47** (2021):32804–32816. DOI: https://doi.org/10.1016/j.ceramint.2021.08.177.

[42] M. Darbandi, M. Eynollahi, N. Badri, M. F. Mohajer, and Z. A. Li. *J. Alloys Compd.*, **889** (2021):161706. DOI: https://doi.org/10.1016/j.jallcom.2021.161706.

[43] F. Moradnia, S. T. Fardood, A. Zarei, S. Heidarzadeh, A. Ramazani, and M. Sillanpää. *Iran. J. Catal.*, **14** (2024), . DOI: https://doi.org/10.57647/j.ijc.2024.1401.01.

[44] F. Motahari, M. R. Mozdianfard, F. Soofivand, and M. Salavati-Niasari. *RSC Adv.*, **4** (2014):27654–27660. DOI: https://doi.org/10.1039/C4RA02697G.

[45] F. Iazdani and A. Nezamzadeh-Ejhieh. *Spectrochim. Acta, Part A*, **250** (2021):119228. DOI: https://doi.org/10.1016/j.saa.2020.119228.

[46] M. Chauhan, N. Kaur, P. Bansal, R. Kumar, S. Srinivasan, and G. R. Chaudhary. *J. Nanomater.*, **2020** (2020):6123178. DOI: https://doi.org/10.1155/2020/6123178.

[47] S. Gadge, A. Tamboli, M. Shinde, H. Fouad, C. Terashima, R. Chauhan, and S. Gosavi. *J. Solid State Electrochem.*, **27** (2023): 2005–2015. DOI: https://doi.org/10.1007/s10008-023-05464-3.

[48] S. R. Shakor, A. Naghipour, and S. T. Fardood. *Case Stud. Chem. Environ. Eng.*, **11** (2025):101076. DOI: https://doi.org/10.1016/j.cscee.2024.101076.

[49] C. Lops, A. Ancona, K. Di Cesare, B. Dumontel, N. Garino, G. Canavese, S. Hérnandez, and V. Cauda. *Appl. Catal., B*, **243** (2019):629–640. DOI: https://doi.org/10.1016/j.apcatb.2018.10.078.

[50] N. Yang, B. M. Jun, J. S. Choi, C. M. Park, M. Jang, A. Son, S. N. Nam, and Y. Yoon. *Chemosphere*, **354** (2024):141676. DOI: https://doi.org/10.1016/j.chemosphere.2024.141676.

[51] S.A. Asli and M. Taghizadeh. *ChemistrySelect*, **5** (2020):13720–13731. DOI: https://doi.org/10.1002/slct.202003612.

[52] P. Qiu, B. Park, J. Choi, B. Thokchom, A. B. Pandit, and J. Khim. *Ultrason. Sonochem.*, **45** (2018):29–49. DOI: https://doi.org/10.1016/j.ultsonch.2018.03.003.

[53] X. Wang, X. S. He, C. Y. Li, S. L. Liu, W. Lu, Z. Xiang, and Y. Wang. *J. Water Process Eng.*, **51** (2023):103345. DOI: https://doi.org/10.1016/j.jwpe.2022.103345.

[54] P. O. Oladoye, M. O. Bamigboye, O. D. Ogunbiyi, and M. T. Akano. *Groundwater Sustainable Dev.*, **19** (2022):100844. DOI: https://doi.org/10.1016/j.gsd.2022.100844.

[55] S. Joulaee, M. Mirzaei, A. Hassanpour, H. Safardoust-Hojaghan, and A. Khani. *Optik*, **290** (2023):171324. DOI: https://doi.org/10.1016/j.ijleo.2023.171324.

[56] A. Selmi, H. Teymourinia, A. Zarei, M. Timoumi, and A. Ramazani. *Iran. J. Catal.*, **12** (2022). DOI: https://doi.org/10.30495/ijc.2022.689626.

[57] S. Taghavi Fardood, F. Moradnia, S. Ganjkhanlu, L. Ouni, A. Ramazani, and M. Sillanpää. *Inorg. Chem. Commun.*, **167** (2024): 112719, . DOI: https://doi.org/10.1016/j.inoche.2024.112719.

[58] E. Abdelkader and L. Nadjia. *Iran. J. Catal.*, **14** (2024). DOI: https://doi.org/10.57647/j.ijc.2024.1404.41.

[59] A. K. Ramasami, M. V. Reddy, and G. R. Balakrishna. *Mater. Sci. Semicond. Process.*, **40** (2015):194–202. DOI: https://doi.org/10.1016/j.mssp.2015.06.017.

[60] A. Singh, V. Goyal, J. Singh, H. Kaur, S. Kumar, K. M. Batoo, J. Gaur, M. Pal, M. Rawat, and S. Hussain. *J. Cleaner Prod.*, **343** (2022):131026. DOI: https://doi.org/10.1016/j.jclepro.2022.131026.

[61] K. Ravindhranath and M. Ramamoorty. *Orient. J. Chem.*, **33** (2017): 1603.
DOI: https://doi.org/10.13005/ojc/330403.

[62] L. Nadjia, E. Abdelkader, B. Naceur, and B. Ahmed. *J. Rare Earths*, **36** (2018):575–587, .
DOI: https://doi.org/10.1016/j.jre.2018.01.004.

[63] N. Mehrabanpour, A. Nezamzadeh-Ejhieh, S. Ghattavi, and A. Ershadi. *Appl. Surf. Sci.*, **614** (2023):156252.
DOI: https://doi.org/10.1016/j.apsusc.2022.156252.

[64] S. Ghattavi and A. Nezamzadeh-Ejhieh. *Catal. Sci. Technol.*, **13** (2023):737–749, .
DOI: https://doi.org/10.1039/D2CY01815B.

[65] S. A. Mirsalari, A. Nezamzadeh-Ejhieh, and A. R. Massah. *Spectrochim. Acta, Part A*, **288** (2023):122139.
DOI: https://doi.org/10.1016/j.saa.2022.122139.

[66] S. Taghavi Fardood, F. Moradnia, and T.M. Aminabhavi. *Environ. Pollut.*, **358** (2024):124534, .
DOI: https://doi.org/10.1016/j.envpol.2024.124534.

[67] S. Taghavi Fardood, F. Moradnia, R. Forootan, R. Abbassi, S. Jalalifar, A. Ramazani, and M. Sillanpaa. *J. Photochem. Photobiol. A: Chem.*, **423** (2022):113621, .
DOI: https://doi.org/10.1016/j.jphotochem.2021.113621.

[68] L. Nirumand, S. Farhadi, A. Zabardasti, and A. Khataee. *Ultrason. Sonochem.*, **42** (2018):647–658.
DOI: https://doi.org/10.1016/j.ultsonch.2017.12.033.

[69] A. Khataee, M. Sheydaei, A. Hassani, M. Taseidifar, and S. Karaca. *Ultrason. Sonochem.*, **22** (2015):404–411, .
DOI: https://doi.org/10.1016/j.ultsonch.2014.07.002.

[70] L. Nadjia, A. Chakib, K. Mohamed, T. Mohamed, and E. Abdelkader. *Appl. Phys. A*, **131** (2025):154, .
DOI: https://doi.org/10.1007/s00339-024-08223-x.

[71] A. Khataee, D. Kalderis, P. Y. Motlagh, V. Binas, S. Stefa, and M. Konsolakis. *J. Ind. Eng. Chem.*, **95** (2021):73–82, .
DOI: https://doi.org/10.1016/j.jiec.2020.12.006.

[72] S. Taghavi Fardood, S. Ganjkhanlu, F. Moradnia, and A. Ramazani. *Sci. Rep.*, **14** (2024):16670, .
DOI: https://doi.org/10.1038/s41598-024-67655-w.

[73] S. Ghattavi and A. Nezamzadeh-Ejhieh. *Compos. B Eng.*, **183** (2020): 107712, .
DOI: https://doi.org/10.1016/j.compositesb.2019.107712.

[74] K. K. Veni, L. C. Nehru, R. Kavitha, and S. Sagadevan. *Surfaces Interfaces*, **51** (2024):104590, .
DOI: https://doi.org/10.1016/j.surfin.2024.104590.

[75] A. Z. Abdullah and P. Y. Ling. *J. Hazard. Mater.*, **173** (2010):159–167.
DOI: https://doi.org/10.1016/j.jhazmat.2009.08.060.

[76] S. A. Bhat, F. Zafar, A. H. Mondal, A. Kareem, A. U. Mirza, S. Khan, A. Mohammad, Q. M. R. Haq, and N. Nishat. *J. Iran. Chem. Soc.*, **17** (2020):215–227.
DOI: https://doi.org/10.1007/s13738-019-01767-3.

[77] D. A. H. Harki, A. Naghipour, and S. Taghavi Fardood. *Case Stud. Chem. Environ. Eng.*, **10** (2024):101016.
DOI: https://doi.org/10.1016/j.cscee.2024.101016.

[78] Y. D. Chai, Y. L. Pang, S. Lim, and W. C. Chong. *Mater. Today:. Proc.*, **42** (2021):50–55.
DOI: https://doi.org/10.1016/j.matpr.2020.09.246.

[79] S. Taghavi Fardood, F. Yekke Zare, F. Moradnia, and A. Ramazani. *J. Rare Earths*, **43** (2025):736–742, .
DOI: https://doi.org/10.1016/j.jre.2024.03.006.